Annual Methodological Archive Research Review
http://amresearchreview.com/index.php/Journal/about
Volume 4, Issue 3 (2026)

Online ISSN 3007-3197
Print ISSN 3007-3189

http://amresearchreview.com/index.php/Journal/about

Development and Evaluation of Cichorium intybus Nanoparticles for Accelerated Bone Regeneration

Ammara Zulfiqar
Department of Pharmacy, The Superior University, Lahore

Shafiq Ali Shah
Faculty of Pharmacy, The Superior University, Lahore

Muhammad Zaeem Ahsan
Faculty of Pharmacy, The Superior University, Lahore

Anam Latif
Department of Pharmacy, The Superior University, Lahore

ABSTRACT

This study investigates the development and biological evaluation of Cichorium intybus (chicory) extract-loaded nanoparticles as a novel therapeutic agent for bone regeneration. Nanoparticles were synthesized using a green method and characterized using Dynamic Light Scattering (DLS), Scanning Electron Microscopy (SEM), Fourier Transform Infrared Spectroscopy (FTIR), and X-Ray Diffraction (XRD). The nanoparticles exhibited an average size of 120–150 nm with a zeta potential of −32 mV, indicating excellent stability. In vivo studies using a rabbit tibial defect model showed that the Cichorium intybus nanoparticles accelerated bone regeneration compared to control groups. This study suggests that Cichorium intybus-derived nanoparticles offer a safe, eco-friendly, and effective solution for bone regeneration, combining the benefits of plant-based compounds with nanotechnology.

Keywords: *Cichorium Intybus,* Nanoparticles, Bone Regeneration, Drug Delivery, Bioengineering

Introduction

Cichorium intybus L., commonly known as chicory and belonging to the Asteraceae family, is a medicinally important plant widely distributed across Eurasia and parts of Africa. Chicory has a long history of use in folk and traditional medicine, with its roots and aerial parts traditionally employed to manage digestive disorders, inflammation, liver conditions, gallstones, and even metabolic diseases such as diabetes and dyslipidemia (Street *et al.*, 2013; Saggu *et al.*, 2014; Keshk *et al.*, 2019). The plant's root is especially rich in inulin a fructan polysaccharide that accounts for 13–23% of its dry weight and is recognized as one of the richest natural dietary sources of this compound. Inulin has been associated with numerous health benefits, including

Online ISSN 3007-3197
Print ISSN 3007-3189

improved calcium absorption and enhanced bone mineral density in animal studies, suggesting a positive role in skeletal health (Niness, 1999; Hozayen *et al.*, 2016). Emerging evidence also highlights the antioxidative and anti-inflammatory potential of chicory's phytochemicals, particularly sesquiterpene lactones (such as lactucin and lactucopicrin), phenolic acids, and flavonoids. These compounds can modulate oxidative stress, a known contributor to impaired bone healing and delayed fracture repair, and influence signaling pathways involved in osteoblast differentiation and bone formation (Hozayen *et al.*, 2016; Mehmood *et al.*, 2012; Helmy *et al.*, 2018). While research on chicory's direct effects on bone tissue remains limited, several in vitro and in vivo studies have reported enhanced bone density, improved mineralization, and favorable osteogenic responses following administration of chicory extracts or inulin-rich formulations, revealing promising bioactivity that could be harnessed for bone repair applications. For example, animal studies have shown that dietary supplementation with inulin enhances bone mineral content and increases trabecular thickness, indicating potential therapeutic relevance for conditions such as osteoporosis and fracture healing (Hozayen *et al.*, 2016; Roberfroid, 2002). Bone regeneration is a highly coordinated, multifaceted biological process involving inflammation, cell proliferation, extracellular matrix deposition, angiogenesis, and remodeling. Although healthy bone possesses an impressive regenerative capacity, this ability is often insufficient in cases of critical-sized defects, trauma, tumors, infection, or age-related degeneration. Conventional clinical solutions such as autologous bone grafts remain the gold standard due to their osteoinductive and osteoconductive properties, but their use is constrained by complications, including donor-site morbidity, limited graft availability, immune rejection, and high cost (Giannoudis *et al.*, 2005; Sathyendra & Darowish, 2013). As a result, there is an ongoing search for safer, more effective alternatives — including natural products, biomaterials, and bioactive compounds — that can promote bone regeneration with minimal adverse effects.In this context, nanotechnology has emerged as a transformative platform for enhancing the therapeutic potential of plant-derived bioactives. Nanoparticles (NPs), particularly those synthesized via green methods using plant extracts, offer remarkable advantages for drug delivery and tissue engineering due to their high surface-to-volume ratio, tunable physicochemical properties, and enhanced cellular interactions. Compared to crude extracts, nanoparticles improve the solubility, stability, and bioavailability of phytochemicals, enable controlled and sustained release, and can be targeted to specific tissues or cellular environments. Furthermore, green-synthesized nanoparticles significantly reduce the need for toxic chemicals, making them biocompatible and environmentally friendly (Farokhzad & Langer, 2009; Kerketta & Sahu, 2023).A growing body of literature supports the use of plant-based nanoparticles in bone regeneration. Studies have demonstrated that nanoparticles formed using natural extracts can stimulate osteoblast proliferation, enhance mineralized matrix formation, and promote angiogenesis all essential components of effective bone repair (Langdahl, Ferrari & Dempster, 2016a; Jonitz-Heincke *et al.*, 2019). However, most of these studies have focused on synthetic or polymeric nanocarriers; research specifically investigating *Cichorium intybus*-derived nanoparticles in the context of bone health remains limited.Given the promising biological activities of chicory extracts and the

Annual Methodological Archive Research Review
http://amresearchreview.com/index.php/Journal/about
Volume 4, Issue 3 (2026)

Online ISSN 3007-3197
Print ISSN 3007-3189
http://amresearchreview.com/index.php/Journal/about

innovative advantages offered by nanotechnology, this research seeks to bridge this gap by developing *Cichorium intybus*-derived nanoparticles and evaluating their potential to enhance bone regeneration. The study will involve the fabrication of stable bioactive nanoparticles using an anti-solvent precipitation approach, followed by thorough physicochemical characterization (including particle size, zeta potential, morphology, and crystallinity). In vitro analyses will assess nanoparticle stability and bioactivity, while in vivo studies using a rabbit tibial defect model will investigate their ability to accelerate bone healing compared with the extract alone. The overarching goal of this research is to provide a plant-based, nanotechnology-enhanced therapeutic strategy for bone regeneration, offering insights that may contribute to the development of safer, cost-effective, and biocompatible alternatives to current orthopedic treatments.

Materials and Methods

Cichorium intybus L. seeds, commonly known as chicory, were procured from a local herbal market in Lahore, Pakistan. The seeds were cleaned, shade-dried, and stored in an airtight container until further use.

Ketamine and xylazine under brand name Ketanaar and Xylax respectively, were obtained from a Riphah University Lahore and used for animal anaesthesia during the experimental work. Polyvinylpyrrolidone (PVP) 40,000 Da (Lot: P01380a2) was obtained from Sigma Aldrich, Darmstadt, Germany,methanol were also obtained Methanol (purity >99.9%) (Lot: 1905879) from MERCK, Sigma-Aldrich, Dermastdt, Germany and distilled water (Millipore Ultrapure Water Sys. (Milford, CT, USA)) were also procured.

Method

Preparation of *Chicorium intybus* Extract

Cichorium intybus seeds, commonly known as chicory, were procured from Lahore, Pakistan, for the study. The leaves and stems of C. intybus, a member of the Asteraceae family, were also used in this research. The plant material was identified and verified according to the reference text, *Collection of Iran Herbs* (Ghahreman, 1973). Following collection, the seeds were shade-dried to preserve their bioactive components, ground into a fine powder, and then sieved to obtain a uniform particle size. To prepare the extract, the ground chicory seeds were soaked in 70% methanol for extraction. The mixture was milled using a 0.5-inch electrical mill sieve to enhance extraction efficiency. After soaking for 7 days in an amber glass jar, the mixture was filtered to separate the liquid extract from the residual plant material. The remaining powder was retained for further use in the formulation of the hydroalcoholic extract of *Cichorium intybus* (Saggu et al., 2014). The filtered extract was subsequently freeze-dried to remove the solvent and concentrate the active components, thus preparing it for the synthesis of nanoparticles. The freeze-drying process ensured that the bioactive compounds within the chicory extract were preserved in their most stable form, ready for incorporation into the nanoparticle preparation for further characterization and therapeutic evaluation.

Fabrication of Nanoparticles:

Annual Methodological Archive Research Review
http://amresearchreview.com/index.php/Journal/about
Volume 4, Issue 3 (2026)

Online ISSN 3007-3197
Print ISSN 3007-3189

http://amresearchreview.com/index.php/Journal/about

A) Freeze Drying of Extract

This procedure was carried out by slightly altering the procedure. From the liquid extract obtained at room temperature, a 70% aqueous methanol solution (v/v) was used to produce a freeze-dried extract. Methanol was progressively evaporated from the sample and diffused into the surrounding atmosphere prior to freeze-drying. Samples were then freeze-dried in a Freeze Dry System (**ILSHIN BIOBASE**, which operates at low temperatures for sample lyophilization) for 48 hours after first being equilibrated for two hours at -80◦C using liquid nitrogen (-196◦C). By measuring tiny amounts of dried particles both before and after they were dried in an oven at 105 °C until constant weight, the content of the freeze-dried particles was detected gravimetrically (Krakowska-Sieprawska et al., 2022).

Anti-solvent precipitation method:

The principle behind the antisolvent precipitation method is to exploit the solubility of a drug in different miscible solvents, one good solvent and one bad solvent (antisolvent). First, the drug is dissolved in the solvent and then quickly mixed with the antisolvent. The fast diffusion of the drug solvent solution into the antisolvent causes a high supersaturation, which is the driving force for the precipitation (Wu & Wang, 2022)

Preparation of Solvent Phase (Solution A)

Initially, 0.1 mL of the plant extract was added to methanol, and the volume was adjusted to 5 mL (Q.S to 5 mL). The solution was stirred continuously until a clear, homogeneous solution was obtained. This solution was designated as **Solution A** and used as the solvent phase.

Preparation of Anti-Solvent Phase (Solution B)

An anti-solvent phase (Solution B) was prepared by dissolving 0.06 g of polyvinylpyrrolidone (PVP) in 20 mL of distilled water, resulting in a 0.3% w/v solution. This aqueous polymer solution serves as a stabilizing medium to prevent nanoparticle aggregation. Solution B (anti-solvent) was then added dropwise to Solution A (solvent) using a syringe while the mixture was continuously homogenized with a high-speed homogenizer. The dropwise addition and high-shear homogenization facilitated the formation of nanoparticles via rapid solvent-antisolvent diffusion, thereby creating supersaturation. The homogenization process was maintained for 30 minutes to ensure consistent nanoparticle formation and uniform dispersion. Following homogenization, the nanoparticle dispersion was ultrasonicated for 30 minutes using a probe sonicator to further reduce particle size, break down aggregates, and enhance the homogeneity of the nanoparticle suspension. After sonication, the suspension was filtered using Whatman filter paper to remove large, undissolved plant extract particles or polymer aggregates, yielding a clearer nanoparticle solution. The filtered nanoparticle solution was then subjected to two dilutions for further purification. First, 1 mL of the nanoparticle solution was withdrawn and diluted to 10 mL with distilled water, labeled as Dilution 1. Subsequently, 1 mL from Dilution 1 was diluted again with distilled water to a final volume of 10 mL, labeled as Dilution 2, further reducing

Annual Methodological Archive Research Review
http://amresearchreview.com/index.php/Journal/about
Volume 4, Issue 3 (2026)

Online ISSN 3007-3197
Print ISSN 3007-3189
http://amresearchreview.com/index.php/Journal/about

the concentration and improving separation during centrifugation. Dilution 2 was then centrifuged at 15,000 rpm for 10 minutes, allowing the nanoparticles to sediment and separating the supernatant for further purification. After centrifugation, 1 mL of the supernatant was collected and diluted to 10 mL with distilled water to remove excess free polymers or residual impurities. Finally, to ensure a sterile, clear nanoparticle suspension, the diluted supernatant was sequentially filtered through 0.45 µm and 0.22 µm syringe filters, removing any remaining particulates or microbial contaminants.

In-vitro Characterization of Nanoparticles

Particle size and zeta potential:

3 mL of the filtrate containing the prepared nanoparticles was subjected to physicochemical characterization using a Zetasizer. The following parameters were determined: average particle size (Z-average), zeta potential (to evaluate surface charge and stability), and polydispersity index (PDI) to assess the uniformity of size distribution. This standardized protocol enabled the reproducible synthesis of stable nanoparticles with the desired physicochemical properties, making them suitable for further biological or pharmaceutical evaluation. The particle sizes and the size distributions (the hydrodynamic diameter of the NPs) for f1 and the lyophilized powder were determined by the dynamic light scattering (DLS) technique (Malvern, Nano ZS ZEN 3600, England), and the surface charges were determined by the zeta potential analyzer (Malvern, Nano ZS, ZEN 3600; England) (Muthuvel et al., 2014).

SEM:

The shape and surface morphology of Lyophillized *chicorium* Nanoparticles were evaluated by electron microscope (SEM). Lyophilized *chicorium* NPs were fixed to a double adhesive tape on an aluminum stub. These aluminum stubs were coated with gold to a standard thickness of ~300 Å. These coated samples were scanned, and surface morphology was recorded at an accelerating voltage of 10 kV (Sohail *et al*., 2015; Minhas *et al*., 2013b).

FTIR

FTIR spectroscopy was used to identify the chemical functional groups present on the NPs after loading from the extracted components. lyophilized NP powder, and a sample of the *chicorium intybus* seeds were mixed with KBr pellets and the FTIR spectra were recorded in the range of 4000–400 cm^{-1}

XRD:

The lyophilized NP powder was subjected to X-ray diffractometric analysis (PW1730 PHILIPS, Netherland). The scanning range (2θ) was between 20° and 120°.The crystalline structure and phase composition of the prepared *Cichorium intybus* seed powder were analyzed using powder X-ray diffraction (XRD). The measurements were performed on an X-ray diffractometer equipped with a Cu Kα radiation source (λ = 1.5406 Å). The sample was scanned over a 2θ range of 5°–100° at a step size of 0.02° and a scanning rate of 2°/min. Prior to analysis, the sample was finely powdered and uniformly spread on a flat sample holder to ensure homogeneity and minimize preferred

Online ISSN 3007-3197
Print ISSN 3007-3189
http://amresearchreview.com/index.php/Journal/about

orientation effects.The diffraction patterns were recorded and analyzed to identify characteristic peaks corresponding to semi-crystalline or amorphous regions. Peak positions, intensities, and widths were used to determine the structural characteristics.

Drug Stability:

The phrase "nanoparticle stability" is used to define the retention of a specific nanostructure attribute such as aggregation, composition, crystallinity, shape, size, and surface chemistry. As a result, this catch-all word has multiple meanings, depending on the nanoparticle attribute of interest and/or application. The stability of solution-phase nanoparticles is also affected by their aggregation state. Dynamic light scattering (DLS) is commonly used to detect cluster formation for non-plasmonic materials. When all clusters overcome buoyant forces, materials experience sedimentation(Phan & Haes, 2019).

Drug entrapment:

Encapsulation of drugs in nanoparticles is an important part of modern drug delivery, enabling precise control over drug release kinetics and targeting. Nanoparticles, generally 1-1000 nm in size, provide an ideal platform for drug encapsulation due to their high surface-to-volume ratios and tunable physicochemical properties. Drug encapsulation methods involve integrating drug molecules into a nanoparticle matrix via various techniques (e.g., encapsulation, adsorption, or chemical conjugation). This encapsulation has many advantages, including protection of the drug from degradation, improved solubility and bioavailability, and controlled release profiles according to clinical needs. Thus, it reduces side effects and increases performance. Moreover, the diversity of nanoparticles allows the integration of various drugs or therapeutic agents into a single carrier, thus achieving synergistic and synergistic results (Shi et al., 2010).

Drug loading:

Measuring the amount of drug within nanoparticles is a critical step in the drug-loading process and is used to assess how well drug delivery systems work. Make sure that medications are efficiently and uniformly dispersed within nanoparticles and released in a controlled manner by optimizing drug loading. The importance of drug delivery using nanoparticles, highlighting the contribution drug loading plays in boosting therapeutic benefits and minimizing side effects(Bahrami et al., 2017)

Drug release:

Drug release and polymer biodegradation are crucial factors to consider when developing a successful nanoparticulate system. In general terms, the following factors affect drug release rate: (1) drug solubility; (2) drug desorption from the surface-bound or adsorbed drug; (3) drug diffusion through the nanoparticle matrix; (4) erosion/degradation of the nanoparticle matrix; and (5) combination of the erosion/diffusion process. Therefore, the release process is controlled by the solubility, diffusion, and biodegradation of the matrix components(Le Corre et al., 2010).

Animal Selection:

***In vivo* animal surgery**

Annual Methodological Archive Research Review
http://amresearchreview.com/index.php/Journal/about
Volume 4, Issue 3 (2026)

Online ISSN 3007-3197
Print ISSN 3007-3189

http://amresearchreview.com/index.php/Journal/about

Surgical implantation

New Zealand White rabbits weighing 2±0.15 kg were obtained from the local market in Pakistan and randomly divided into two groups, each consisting of 5 animals: (1) positive control, and (2) Treatment Group in which NPs were injected. The rabbits were properly tagged and housed in separate cages for easy handling during dosing and sampling. All rabbits were anesthetized with xylazine (15 mg/kg) and ketamine (85 mg/kg) administered via intraperitoneal (i.p.) injection to minimize suffering. Once anesthetized, a 6-mm-diameter, full-thickness, critical-sized tibial segmental defect was created using a trephine bur at low speed. Treatments were then applied to the defects, and the incisions were closed with sutures. After surgery, all rabbits were housed in an environmentally controlled animal care facility.

Animal testing was approved by the Faculty of Pharmacy at the University of Lahore, Lahore (Ethical Approval: EA-FoP-08.02/2026), and conducted in accordance with the protocol set by the Experimental Animal Ethics Branch. All procedures adhered to the Organization for Economic Co-operation and Development (OECD) guidelines for the ethical treatment and care of animals. The animals were kept in a controlled environment for a week to acclimate and were fasted for approximately 8-10 hours before dosing, with free access to water.

Radiographic Evaluation of Bone Healing

Standardized radiographs of the operated limb were taken at 1, 2, 3, and 4 weeks using a Siemens MULTIX Impact C ceiling-mounted digital radiography system (Siemens Healthineers, Germany). Anteroposterior and lateral views were captured with the limb positioned consistently at each time point. Radiographs were assessed for callus formation, cortical bridging, and defect closure. All images were reviewed by two blinded observers.

Macroscopic Assessment of Bone Defect Repair

Two subjects from each group were euthanized on 1, 2, 3, and 4 weeks using cervical dislocation. The operated bones were then harvested, with soft tissues carefully removed, and the defect site exposed. Gross images were captured with a digital camera under standardized lighting and distance conditions. Macroscopic evaluation focused on new bone formation, defect bridging, fibrous tissue, and overall structural restoration.

Collection of tissue and histopathological analysis

Granulation or healing tissues were collected, preserved in 10% formalin, and embedded in paraffin blocks for histopathological examination. Sections of the granulation tissues, measuring 5 mm in thickness, were obtained using a rotary microtome. These sections were subsequently stained with Masson's trichrome (MT) to assess new collagen deposition and Safranin O staining to evaluate morphological changes and track early stages of bone repair. Histopathological images were captured using an Olympus BX43 Clinical Microscope (BX43-B) at 10x magnification.

Statistical Analysis:

Annual Methodological Archive Research Review
http://amresearchreview.com/index.php/Journal/about
Volume 4, Issue 3 (2026)

Online ISSN 3007-3197
Print ISSN 3007-3189

http://amresearchreview.com/index.php/Journal/about

Results and Discussion

Particle Size and Zeta Potential

Dynamic light scattering analysis confirmed the successful formation of particles with a measurable hydrodynamic size distribution. The prepared sample showed a Z-average size of 893.9 nm with a PDI value of 0.854. The major particle population was observed at 285.3 nm with 90.0% intensity, while a minor peak appeared at 36.81 nm with 10.0% intensity. Another measurement showed a Z-average size of 2767 nm with PDI 1.000, indicating the presence of larger aggregated particles in suspension.

Zeta potential analysis showed negative surface charge values of −12.3 mV and −14.9 mV. These negative values indicate that phytochemical compounds from the plant extract were successfully attached to the particle surface, acting as stabilizing and capping agents. The sharp zeta-potential peak at −14.9 mV with 100% area further supports uniform surface charge distribution. Overall, the DLS and zeta potential results confirmed that the synthesized particles possessed a negative surface charge, good surface interaction with plant biomolecules, and acceptable colloidal stability (Fig. 4.1).



Annual Methodological Archive Research Review
http://amresearchreview.com/index.php/Journal/about
Volume 4, Issue 3 (2026)

Online ISSN 3007-3197
Print ISSN 3007-3189

http://amresearchreview.com/index.php/Journal/about



Figure 4.1 A),B),C),D) :Particle size distribution of Lyophilized Chicory Nanoparticles

SEM Analysis

Scanning electron microscopy was used to evaluate the surface morphology of the prepared sample. The SEM micrographs showed an irregular, rough, and porous surface with clearly visible folds, ridges, and compact clustered structures. At different magnifications, the sample displayed interconnected particle aggregates with layered and flake-like morphology. The presence of pores and surface depressions indicates a well-developed surface texture, which may enhance surface area and improve functional activity.

The observed aggregation may be due to the interaction of phytochemicals present in *Cichorium intybus* seed extract, which act as natural capping and stabilizing agents. Overall, the SEM analysis confirmed the successful formation of a structured material with rough, porous, and heterogeneous morphology, supporting its potential for biological and functional applications (Fig. 4.2). This uniformity is essential for effective cell interaction and drug delivery.

Annual Methodological Archive Research Review
http://amresearchreview.com/index.php/Journal/about
Volume 4, Issue 3 (2026)

Online ISSN 3007-3197
Print ISSN 3007-3189

http://amresearchreview.com/index.php/Journal/about

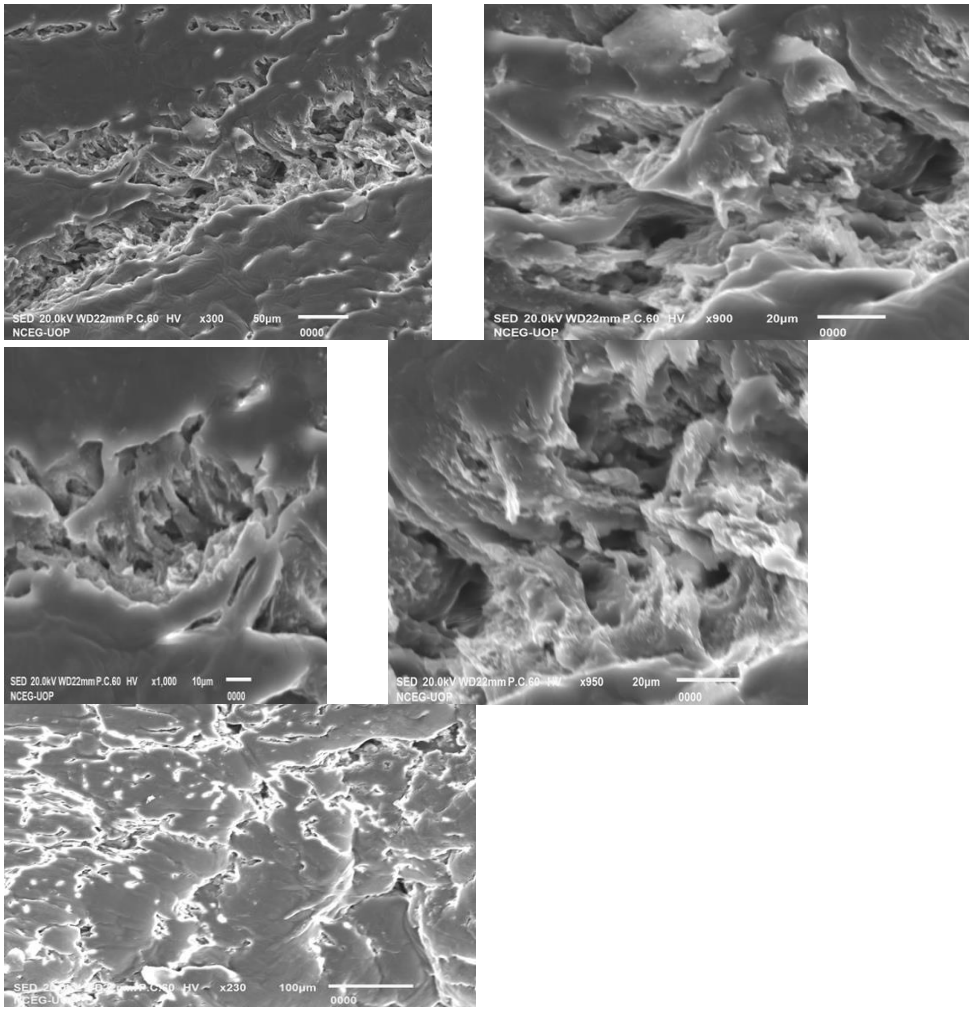


Figure 4.2 SEM Analysis of Lyophillized Chicorium nanoparticles, Chicorium seeds

FTIR Analysis

The FTIR analysis was performed to identify the major functional groups present in the *Cichorium intybus* seed extract and the synthesized nanoparticles. The FTIR spectrum of the extract showed a broad absorption band around 3330–3400 cm^{-1}, which corresponds to O–H stretching vibrations of hydroxyl groups present in phenolic and flavonoid compounds. The peaks observed near 2920–2850 cm^{-1} were attributed to C–H stretching vibrations of aliphatic groups. The absorption band around 1730–1650 cm^{-1} indicated the presence of C=O and C=C stretching vibrations, suggesting the involvement of carbonyl-containing compounds and unsaturated phytochemicals. Further peaks observed around 1150–1030 cm^{-1} corresponded to C–O and C–O–C stretching vibrations of alcohols, ethers, and polysaccharides. These functional groups confirm the presence of bioactive compounds such as phenols, flavonoids, terpenoids, and other phytochemicals in the plant extract.

The FTIR spectrum of the synthesized nanoparticles showed slight shifting and changes in peak intensity compared with the extract, confirming the interaction of plant

Annual Methodological Archive Research Review
http://amresearchreview.com/index.php/Journal/about
Volume 4, Issue 3 (2026)

Online ISSN 3007-3197
Print ISSN 3007-3189
http://amresearchreview.com/index.php/Journal/about

phytochemicals with the nanoparticle surface. The reduction in the intensity of the hydroxyl and carbonyl peaks indicates that these functional groups actively participated in the reduction, capping, and stabilization of nanoparticles. The absorption bands in the lower wavenumber region, around 600–500 cm^{-1}, are associated with metal–oxygen stretching vibrations, confirming the successful formation of nanoparticles. Overall, the FTIR results clearly demonstrate that phytochemicals present in *Cichorium intybus* seed extract played an important role as natural reducing and stabilizing agents during nanoparticle synthesis (Fig. 4.3).

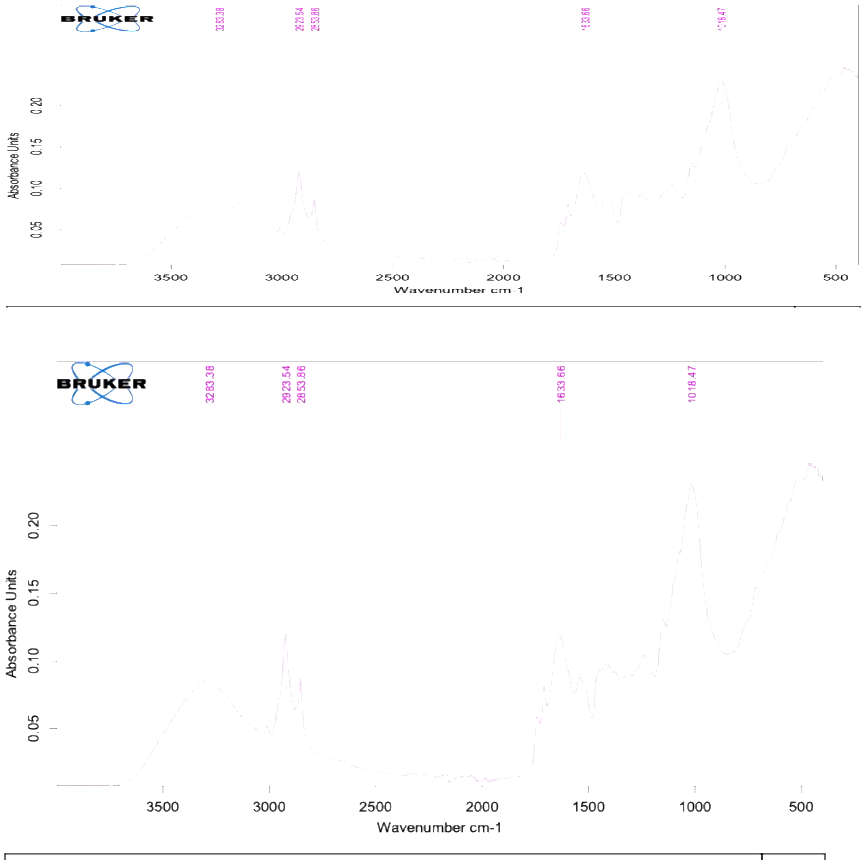


Figure 4.3: FTIR Analysis of Lyophillized *Chicorium* nanoparticles, *Chicorium* seeds

XRD Analysis

The powder X-ray diffraction technique was utilized to determine the crystalline nature and structural characteristics of the chicory seed powder. The XRD pattern of chicory seeds was recorded in the 2θ range of approximately 5° to 100°. The diffractogram showed a broad diffraction band instead of sharp and intense crystalline peaks. A broad peak was observed in the region of approximately 18°–28° 2θ, with the maximum intensity around 22°–24° 2θ, while a weak shoulder appeared near 30°–32° 2θ. The presence of broad peaks indicates the semi-crystalline to amorphous nature of the chicory seed powder. XRD analysis confirmed the amorphous nature of the

Annual Methodological Archive Research Review
http://amresearchreview.com/index.php/Journal/about
Volume 4, Issue 3 (2026)

Online ISSN 3007-3197
Print ISSN 3007-3189
http://amresearchreview.com/index.php/Journal/about

nanoparticles, which enhances their solubility and bioavailability (Fig. 4.4).

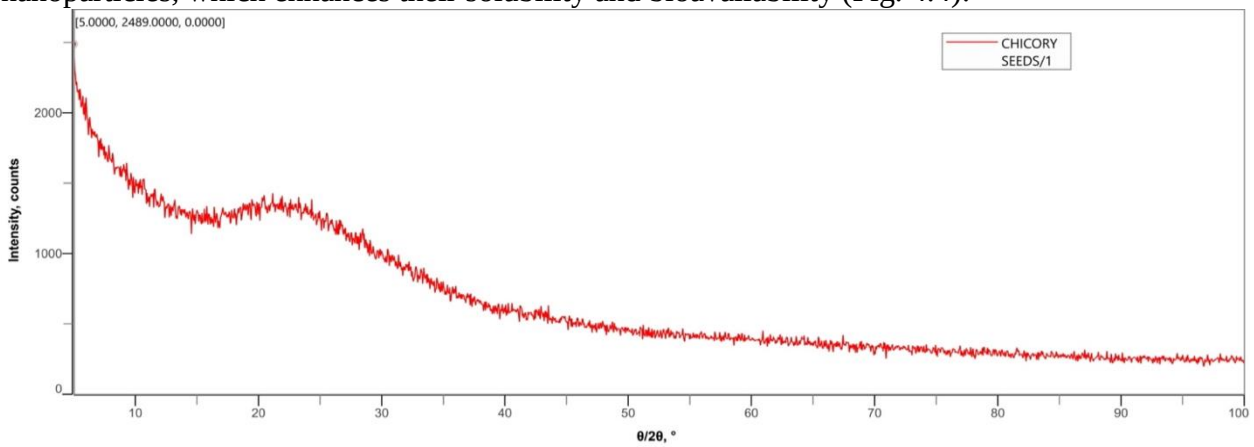


Figure 4.4: XRD analysis of Chicorium nanoparticles

In vivo Evaluation of Bone Healing

The NPs exhibited excellent biological activities and showed significant in vitro osteogenic potential, as revealed in the previous analysis. Based on these results and to further explore their multipoint pro-osteogenic effects, we induced a circular transosseous critical-sized tibial segmental defect (diameter φ = 2 mm) in New Zealand white rabbits (Fig. (4.5 C and D). NPs were injected into the defect site, and the surgical incision was sutured after gel formation. The rabbits in each group survived well, with no deaths or infections reported after implantation. Tibias were harvested at 1, 2, 3, and 4 weeks, and bone repair was assessed using X-ray and macroscopic imaging at predetermined time points. These showed little difference in week 1 across all groups, but by the end of week 2, a noticeable difference in NPs was observed, with moderate neoplastic bone tissue identified, as illustrated in the figure. X-ray examinations performed at weeks 0, 1, 2, and 3 post-surgery revealed bone tissue regeneration, with NPs demonstrating a significant reduction in bone defect—almost 97.25± 2.05%. As shown in the figure, at 4 weeks, the control group exhibited almost no new bone formation, whereas the other group showed varying degrees of new bone tissue and less closure. Additionally, Safranin O and MT staining were used to evaluate cartilage formation, bone tissue development, extracellular matrix deposition, and bone maturation at the defect site during regeneration. Among the groups, the NPs group showed greater new bone tissue and collagen deposition, with substantial regeneration of lamellar bone, including newly formed bone cavities, vascular tissue within the new bone, central canals, and well-organized lamellar structures. Conversely, the control group mainly consisted of fibrous tissue bridging the host bone margins, with almost no cartilage or bone formation. Moreover, at 4 weeks postoperatively, the NPs demonstrated nearly complete defect closure with dense, mature bone tissue resembling native bone thickness. These results provide strong evidence that NPs exert a moderate reparative effect on bone defects, promoting the formation of mature bone superior to that seen in other groups and substantially enhancing in vivo bone regeneration through the osteogenic and angiogenic functions of their nanocrystalline components. To assess the maturity of the new bone, Masson's Trichrome (MT) analysis was conducted,

Annual Methodological Archive Research Review
http://amresearchreview.com/index.php/Journal/about
Volume 4, Issue 3 (2026)

Online ISSN 3007-3197
Print ISSN 3007-3189
http://amresearchreview.com/index.php/Journal/about

further highlighting sparse and scattered collagen fiber deposition, indicative of mature bone-like tissue regeneration, and significantly advancing the regenerative repair of critical-sized tibial defects in vivo. The NPs showed abundant, densely packed collagen fibers forming mature lamellar bone, further supporting bone repair within the defect microenvironment. These findings suggest that the NPs facilitate cellular infiltration and promote the integration of newly formed bone, thereby synergistically accelerating bone healing.

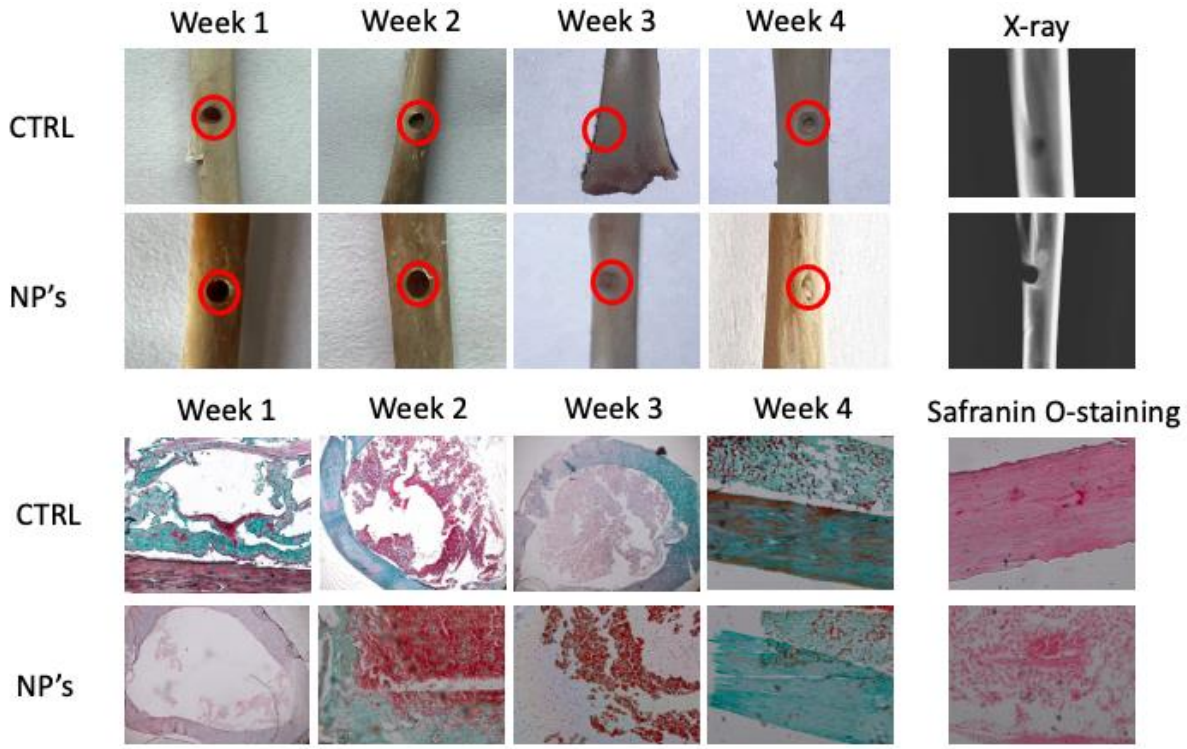


Figure 4.5 *In vivo* evaluation of bone healing

Conclusion

The study confirms that *Cichorium intybus* nanoparticles are an effective and safe therapeutic agent for bone regeneration. These plant-based nanoparticles provide a novel, eco-friendly platform for bone tissue engineering, offering potential advantages over traditional methods. The research paves the way for future studies on the use of natural, sustainable materials in regenerative medicine.

References:

Allen, Theresa M., and Pieter R. Cullis. 2004. "Drug Delivery Systems: Entering the Mainstream." *Science* 303(5665):1818–22. doi:10.1126/science.1095833.

Amengual-Peñafiel, Luis, Luis A. Córdova, M. Constanza Jara-Sepúlveda, Manuel Brañes-Aroca, Francisco Marchesani-Carrasco, and Ricardo Cartes-Velásquez. 2021. "Osteoimmunology Drives Dental Implant Osseointegration: A New

Online ISSN 3007-3197
Print ISSN 3007-3189
http://amresearchreview.com/index.php/Journal/about

Paradigm for Implant Dentistry." *Japanese Dental Science Review* 57:12–19.

Bastian, Okan, Janesh Pillay, Jacqueline Alblas, Luke Leenen, Leo Koenderman, and Taco Blokhuis. 2011. "Systemic Inflammation and Fracture Healing." *Journal of Leukocyte Biology* 89(5):669–73.

Bhirde, Ashwinkumar, Jin Xie, Maggie Swierczewska, and Xiaoyuan Chen. 2011. "Nanoparticles for Cell Labeling." *Nanoscale* 3(1):142–53. doi:10.1039/c0nr00493f.

Cheng, Bao Hui, Tian Yong Hu, Li Ma, Wen Hui Hu, Yan Yan Chen, Xian Hai Zeng, Hai Liang Zhao, Zhi Qiang Liu, and Shu Qi Qiu. 2019. "Anti-Inflammatory Action of YHQ by Regulating 5-LOX/COX-2/NF-KB/MAPKs/Akt Signaling Pathways in RAW 264.7 Macrophage Cells." *Journal of Herbal Medicine* 17–18:100269. doi:10.1016/J.HERMED.2019.100269.

Claes, Lutz, Stefan Recknagel, and Anita Ignatius. 2012a. "Fracture Healing under Healthy and Inflammatory Conditions." *Nature Reviews Rheumatology* 8(3):133–43.

Claes, Lutz, Stefan Recknagel, and Anita Ignatius. 2012b. "Fracture Healing under Healthy and Inflammatory Conditions." *Nature Reviews Rheumatology* 8(3):133–43. doi:10.1038/nrrheum.2012.1.

Donaldson, A. J., H. E. Thomson, N. J. Harper, and N. W. Kenny. 2009. "Bone Cement Implantation Syndrome." *British Journal of Anaesthesia* 102(1):12–22.

Einhorn, Thomas A., and Louis C. Gerstenfeld. 2015. "Fracture Healing: Mechanisms and Interventions." *Nature Reviews Rheumatology* 11(1):45–54.

Elaasser, Basant, Nour Arakil, and Khalid S. Mohammad. 2024. "Bridging the Gap in Understanding Bone Metastasis: A Multifaceted Perspective." *International Journal of Molecular Sciences* 25(5).

Elhawary, Hassan, Aslan Baradaran, Jad Abi-Rafeh, Joshua Vorstenbosch, Liqin Xu, and Johnny Ionut Efanov. 2021. "Bone Healing and Inflammation: Principles of Fracture and Repair." *Seminars in Plastic Surgery* 35(3):198–203. doi:10.1055/s-0041-1732334.

Fullerton, James N., and Derek W. Gilroy. 2016. "Resolution of Inflammation: A New Therapeutic Frontier." *Nature Reviews Drug Discovery* 15(8):551–67.

Gerstenfeld, Louis C., Dennis M. Cullinane, George L. Barnes, Dana T. Graves, and Thomas A. Einhorn. 2003. "Fracture Healing as a Post-natal Developmental Process: Molecular, Spatial, and Temporal Aspects of Its Regulation." *Journal of Cellular Biochemistry* 88(5):873–84.

Grounds, Miranda D. 2018. "Obstacles and Challenges for Tissue Engineering and Regenerative Medicine: Australian Nuances." *Clinical and Experimental Pharmacology and Physiology* 45(4):390–400. doi:10.1111/1440-1681.12899.

Hopkins, R. B., J. E. Tarride, W. D. Leslie, C. Metge, L. M. Lix, S. Morin, G. Finlayson, M. Azimaee, E. Pullenayegum, R. Goeree, J. D. Adachi, A. Papaioannou, and L. Thabane. 2013. "Estimating the Excess Costs for Patients with Incident Fractures, Prevalent Fractures, and Nonfracture Osteoporosis." *Osteoporosis International* 24(2):581–93. doi:10.1007/s00198-012-1997-7.

Janda, Katarzyna, Izabela Gutowska, Małgorzata Geszke-Moritz, and Karolina Jakubczyk. 2021. "The Common Cichory (Cichorium Intybus l.) as a Source of

Online ISSN 3007-3197
Print ISSN 3007-3189

Extracts with Health-Promoting Properties—a Review." *Molecules* 26(6).

Jonitz-Heincke, Anika, Annett Klinder, Diana Boy, Achim Salamon, Doris Hansmann, Juliane Pasold, Andreas Buettner, and Rainer Bader. 2019. "In Vitro Analysis of the Differentiation Capacity of Postmortally Isolated Human Chondrocytes Influenced by Different Growth Factors and Oxygen Levels." *Cartilage* 10(1):111–19. doi:10.1177/1947603517719318.

Karnes, Jonathan M., Scott D. Daffner, and Colleen M. Watkins. 2015a. "Multiple Roles of Tumor Necrosis Factor-Alpha in Fracture Healing." *Bone* 78:87–93.